"Packed Bed Thermal Storage Models for Solar Air Heating and Cooling Systems," *Trans. ASME. J. Heat Transfer* 98-336, (1976).

[5] Mumma,S.A., and Marvin, W.C., "A Method of Simulating the Performance of a Pebble Bed Thermal Energy Storage and Recovery System," *ASME* paper 76-HT-73, ASME/AICHE National Heat Transfer Conf., St. Louis, August, 1976.

[6] Sowell, E.F., and Curry, R.L., "A Convolution Model of Rock Bed Thermal Storage Units," *Solar Energy*, vol. 24, no. 5, pp. 441-449, 1980.

[7] Ammar, A.S.A., Okaz, A.M., Sorour, M.M., and Ghoneim, A.A., "Efficient Collection and Storage of Solar Energy," *Solar & Wind Technology*, vol. 6, no. 6, pp.643-652, 1989.

[8] Van Koppen, C.W., "The Actual Benefits of Thermally Stratified Storage in a Small and a medium Size Solar," *Proceedings ISES*, Atlanta, 1979.

[9] Donald, R., "*Solar Energy*," Prentice-Hall 1981.

[10] Klein, S.A., et al., A Transient Simulation Program," *University of Wisconsin-Madison*, Version 12.2, 1988.

[11] Rohsenow, W.M., Hartnett, J.P., Ganic, E.N., *Handbook of Heat Transfer Fundamentals*, 2nd edition, New York, 1985.

[12] Dittus, F.W., and Boelter, L.M.K., University of California (Berkeley), Pub. Eng., Vol. 2, pp. 443, 1980.

EXPERIMENTAL AND THEORETICAL INVESTIGATION OF THE TRANSIENT RESPONSE OF HYDRAULIC VALVE CONTROLLED ACTUATORS

M.G. Rabie, M.A. Awad, E.I. Imam and N.A. Gadallah
Military Technical College,
Cairo, Egypt.

ABSTRACT

The transient response of hydraulic cylinders controlled by directional control valves through relatively long transmission lines is investigated theoretically and experimentally. A nonlinear mathematical model of the system is developed. The transmission line is described by lumped parameter models assuming different numbers of fluid lumps. The proposed models are validated by comparing the predicted transient responses with experimental results and definite conclusions concerning the optimum number of lumps representing the transmission line. The developed simulation program can be used for the optimization of the system parameters as well as the analysis of the dynamic behavior of the value controlled actuators.

NOMENCLATURE

A_c Piston area, m^2.
A_v Directional control valve opening area, m^2.
B Bulk modulus of oil, Pa.
B_e Equivalent bulk modulus of hydraulic line, Pa.
C Hydraulic capacitance, m^5/N.
C_D Discharge coefficient.
D Line diameter, m.
E Modulus elasticity of pipe wall, N/m^2.
e Poisson's ratio.
F_{ex} Loading force, N.
F_R Piston seat reaction, N.
f Viscous friction coefficient, Ns/m.
f_c Equivalent structural damping of seat material, Ns/m.
h Pipe wall thickness, m.
I Hydraulic inertia, kg/m^4.
i Number of lumps.
L Transmission line length, m.
m_p Mass of piston and moving parts, kg.
K_c Equivalent stiffness of piston seat, N/m.
P_c Cylinder inner pressure, pa.
P_p Inlet pressure, pa.
Q_v Flow through the DCV restriction, m^3/s.
R Hydraulic resistance, Ns/m^5.
t Time, s.
V Volume of oil in the line, m^4.
V_c Minimum volume of oil in the cylinder, m^3.
x Directional control valve spool displacement, m.
y Piston displacement, m.
y_o Maximum piston displacement, m.
y_d Maximum piston seat deformation,m.
μ Oil dynamic viscosity, Pa s.
ρ Oil density, kg/m^3.

SUBSCRIPTS

1 First oil lump
2 Second oil lump
3 Third oil lump
4 Fourth oil lump

INTRODUCTION

The hydraulic power transmission systems are widely applied in different domains due to the advantages of high power to weight ratio and high precision. These systems operate mostly in transient conditions due to the continuous starting and stopping of their hydraulic motors. Therefore, it is necessary to study not only their steady state behavior but also their dynamic characteristics.

A basic subsystem of hydraulic control systems consists of a hydraulic cylinder controlled by means of

a directional control valve through transmission lines. When dealing with the dynamics of such subsystem, special attention should be paid to the evaluation of the transmission line behavior and its effect on the whole system response.

The basic equations of fluid dynamics were developed by Stokes and Navier around 1850. Since that time, the performance of hydraulic transmission lines has been investigated in numerous publications. The usually used distributed parameter models of lines contain partial differential equations and necessitate relatively complicated mathematical analysis.

A simple hydraulic power system includes several transmission lines. The representation of the transmission lines by distributed parameter model complicates the overall system model and makes its solution practically impossible. Therefore, a more simple mathematical model of the transmission lines is needed.

Karnopp [1], proposed a single lump model of hydraulic transmission line. Rabie [2], developed lumped parameter models of different number of lumps and predicted the transient and frequency responses of the transmission lines. The proposed model were validated by comparing the theoretical results with published experimental results. Kassem et al [3], presented a study for the performance of hydraulic transmission lines considering both of the distributed and lumped parameter methods. They concluded that representing the closed end line with four lumps can predict with good precision the response of the line whenever the exciting frequency is less than 3.5 times the line natural frequency.

Most of the previous investigations of the valve controlled hydraulic actuators, such as [4] & [5], dealt with lines of large diameters. The inertia of lines, being negligibly small, is either neglected or added to that of the moving parts. The effect of fluid compressibility is accounted for by adding the volume of fluid line to the volume of the actuator chamber connected to it.
The line is thus represented by a simple resistance.

Arafa and Kassem [6], verified that the resulting model, in this case, would not yield accurate prediction of the system performance when the fluid line inertia is high. They derived the set of equations governing the system dynamics and reduced it to a linear form. Solving the obtained set of linearized equations, using Laplace transformation, they showed that the fluid line inertia might improve the system step response. They showed also that the fluid frictional resistance is of minor effect on the response, since its value is much smaller than that of the control valve. The obtained results are qualitative since the analysis is based on linearized model and is made for a system with certain physical parameters. Kassem [7], presented a generalized analysis for the response of hydraulic actuators to step opening of the control valves considering both of the fluid inertia and compressibility of the transmission lines. Herein, the static and dynamic performance of a hydraulic system consisting from a 4/3 directional control valve, a transmission line and a single acting hydraulic cylinder is investigated experimentally and theoretically. The study is directed to develop a simulation program of the system and validate it through an original experimental work.

MODELLING AND SIMULATION OF THE SYSTEM

System Description

The studied system, Figure (1), consists of a single rod hydraulic cylinder (6) controlled by a pilot operated directional control valve (4). The system is supplied by the hydraulic power by means of a hydraulic power supply unit consisting of a pump (1), an accumulator (2), a relief valve (3) and a bleed off valve (8).

Hydraulic power Supply Unit

In this study the hydraulic power supply unit is looked at as a source of pressure. It acts to deliver the hydraulic liquid at the required constant pressure level. But, in the transient conditions of the system operation the supply pressure is found to be slightly varied. Therefore, the transient pressure variation; $P_p^{(t)}$, is recorded and introduced in the simulation program.

Directional Control Valve

A four way three position pilot operated directional control valve is used. The valve is operated electrically by means of DC solenoids. The flow rate through this valve is given by the following equation.

$$Q_v = C_D A_v (x)\sqrt{2(P_p - P_1)/\rho} \qquad (1)$$

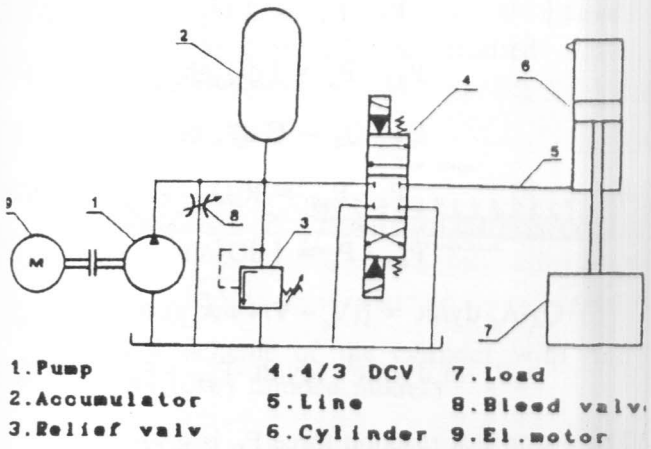

Figure 1. Hydraulic circuit of the studied system.

The spool of the used DCV is of overlapping type. The dependence of the valve opening area on the spool displacement is calculated and presented in Figure (2). The dynamic behavior of the DCV is not investigated in detail in this work, but the transient response of the spool displacement x is evaluated experimentally. A representative model of the valve is deduced on the basis of the experimental results and used for the further analysis of the system.

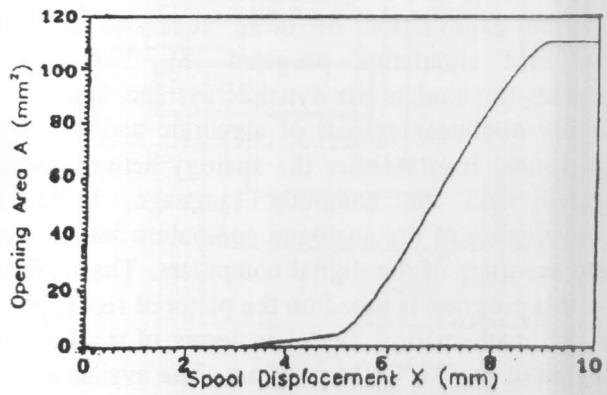

Figure 2. Variation of the throttling area with the spool displacement.

Transmission line

In this study, the transmission line is represented by mathematical models assuming lumped fluid parameters. These models take into consideration the effect of hydraulic resistance, fluid inertia and compressibility.

According to the lumped parameter approach, the effect of the frictional resistance of the whole line is assumed to be lumped in the first portion of line, the effect of line inertia takes place in the second portion while the effect of line elasticity and fluid compressibility is considered in the third portion, Figure (3). The accuracy in representing the line characteristics differs by changing the number of fluid lumps and by interchanging the location of these portions [3].

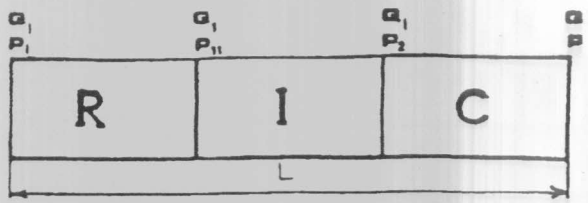

Figure 3. Transmission line with localized effect of resistance, inertia and capacitance.

When deducing the mathematical relations describing the line, the following assumptions are considered.

- The flow in the line is laminar unidirectional.
- The fluid is assumed to move as one or several fluid lumps.
- The parameters of each of the consequent lumps of the line are evaluated by the average flow velocity and average pressure at each section.

Considering a single moving oil lump, Figure (3), the following relations are deduced.

$$P_1 - P_{11} = \frac{128\mu L}{\pi D^4} Q_1 = R Q_1 \qquad (2)$$

$$P_{11} - P_2 = \frac{4\rho L}{\pi D^4}\frac{dQ_1}{dt} = I\frac{dQ_1}{dt} \qquad (3)$$

$$Q_1 - Q_2 = \frac{V}{B} = \frac{V}{B_e}\frac{dP_2}{dt} = C\frac{dP_2}{dt} \qquad (4)$$

where

$$B_e = 1/[\frac{1}{B} + \frac{D}{hE}(0.8 - e)] \quad (5)$$

Figure (4) shows the line represented by more than one lump. The convenient number of lumps representing a line should be determined in view of the required accuracy. The hydraulic resistance, inertia and capacitance of each lump are then given by the following relations.

$$R = \frac{128\mu L/i}{\pi D^4}, I = \frac{4\rho L/i}{\pi D^2} \quad \text{and} C = \frac{\pi d^2 L/i}{4B_e} \quad (6)$$

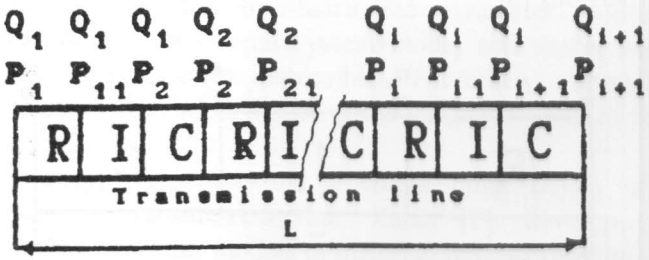

Figure 4. Transmission line represented by i fluid lumps.

MATHEMATICAL MODEL

A scheme of the studied system is shown in Figure (5). The system includes a single rod hydraulic cylinder of perfect internal tightness. This cylinder is mounted vertically and loaded by a constant weight. This system may be described by different mathematical models according to the number of oil lumps. Figure (6) shows schemes of the system with the line represented by one and four oil lumps added to that of the cylinder chamber. In the case of four lumps model, the system behavior is described by the following equations.

$$Q_v = C_D A_v(x)\sqrt{2(P_p - P_1)/\rho} \quad (7)$$

$$Q_v - Q_1 = C\, dP_1/dt \quad (8)$$

$$P_1 - P_{11} = R\, Q_1 \quad (9)$$

$$P_{11} - P_2 = I\, dQ_1/dt \quad (10)$$

$$Q_1 - Q_2 = C\, dP_2/dt \quad (11)$$

$$P_2 - P_{22} = R\, Q_2 \quad (12)$$

$$P_{22} - P_3 = I\, dQ_2/dt \quad (13)$$

$$Q_2 - Q_3 = C\, dP_3/dt \quad (14)$$

$$P_3 - P_{33} = R\, Q_3 \quad (15)$$

$$P_{33} - P_4 = I\, dQ_3/dt \quad (16)$$

$$Q_3 - Q_4 = C\, dP_4/dt \quad (17)$$

$$P_4 - P_{44} = R\, Q_4 \quad (18)$$

$$P_{44} - P_c = I\, dQ_4/dt \quad (19)$$

$$Q_4 - A_c\, dy/dt = [(V_c + V/4 + A_c y)/B]\, dp_c/dt \quad (20)$$

$$A_c P_c - m_p d^2y/dt^2 - f dy/dt - F_{ex} + F_R = 0 \quad (21)$$

The piston seat reaction force F_R is given by:

$$F_R = K_c(y_d - y) + f_c dy/dt \quad \text{for } y \le y_d$$

$$F_R = 0 \quad \text{for } y_o > y > y_d$$

$$F_R = -K_c(y - y_o) \quad \text{for } y \ge y_o$$

SYSTEM SIMULATION

The studied system is described mathematically by equation 7 to 21. The system simulation is carried out by the exploitation of these equations using the TUTSIM simulation program [8]. This program enables to simulate the dynamic systems described by highly nonlinear system of algebraic and differential equations. It establishes the analogy between the real system and the computer language. It has the convenience of the analogue computers and the speed and accuracy of the digital computers. The simulation by this program is based on the pictorial representation of the mathematical model in terms of the functional blocks of the TUTSIM program. The available blocks enable to take into consideration all of the system nonlinearities as well as the generation of the recommended inputs. The constructional and operational parameters of the system have been evaluated by direct measurements on the elements of the system.

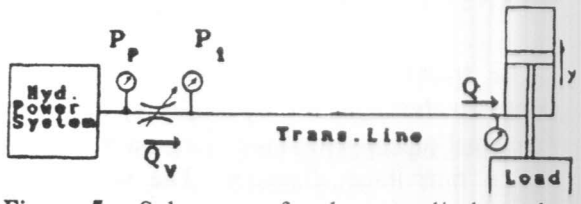

Figure 5. Scheme of the studied valve controlled actuator.

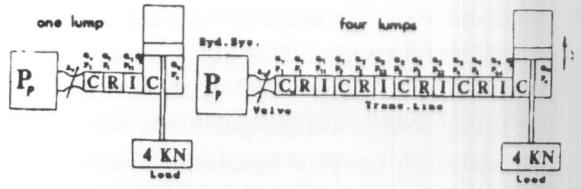

Figure 6. Scheme of the cylinder with line represented by lumped model.

EXPERIMENTAL WORK

The experimental work aims at the evaluation of the validity of the proposed models. The test rig built for this purpose is illustrated in Figure (7) and the following experiments were carried out.

1. Measurement of the transient response of the directional control valve spool displacement and the associated inlet pressure variation.
2. Measurement of the hydraulic resistance and transient response of the transmission line.
3. Measurement of the transient response of the valve controlled actuator.

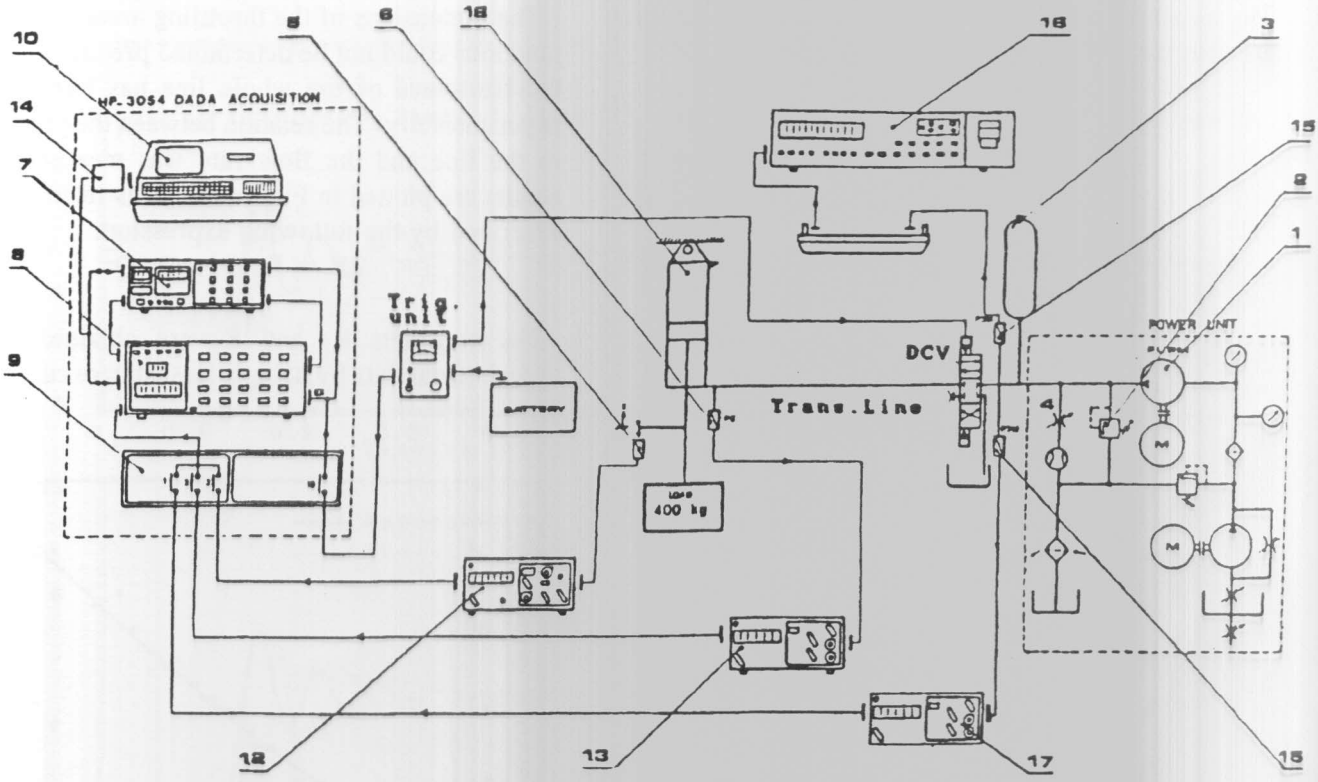

Figure 7. Layout of the test rig hydraulic system.

TRANSIENT RESPONSE OF THE DIRECTIONAL CONTROL VALVE

The system operation is controlled by means of a pilot operated directional control valve. The transient response of this valve depends, in general, on the value of the input pressure. The effect of this pressure on the spool displacement was evaluated experimentally by measuring the transient displacement of the spool at different input pressure levels. The input pressure is found to vary during the transient period, therefore the transient variation of this pressure is also recorded. The experimental results are shown in Figure (8). This figure shows that the variation of the input pressure level in the range from 7.5 to 12.5 MPa has no significant effect on the spool transient response. Therefore, the recorded response, at P_p = 7.5 MPa, is introduced in the simulation program to represent the behavior of the directional control valve. The measured transient variations of the inlet pressure are also introduced in the simulation program.

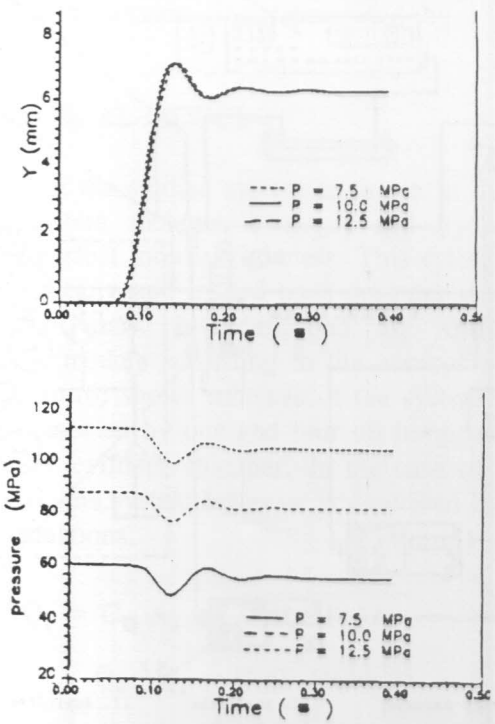

Figure 8. Transient response of the spool displacement of the directional control valve at different pressure levels.

TRANSMISSION LINE HYDRAULIC RESISTANCE

The transmission line, connecting the directional control valve with the hydraulic cylinder, consists of five steel pipes welded together, each is of 3 m length and 6 mm inner diameter. The welding introduces local losses at the junction points due to the reduction of pipe cross-sectional area. The prediction of the resistance of the line by equation (2) did not give satisfactory results when comparing the theoretical and experimental results. This equation counts only for the friction losses. The local losses resulting from the throttling at the welded junctions are not taken into consideration by this equation. The local losses are calculated by the following expressions.

$$\Delta P = \sum \xi \rho v^2/2 \text{ or } \Delta P = R_2 Q^2 \qquad (24)$$

The dimensions of the throttling areas at the welding junctions could not be determined precisely, therefore, the resistance of the whole line has been found out experimentally. The relation between the pressure drop in the line and the flow rate was measured and the results are plotted in Figure (9). This relation could be described by the following expression.

$$\Delta P = R_1 Q + R_2 Q^2 \qquad (25)$$

The constants R_1 and R_2 are obtained from the experimental data by using a least square curve, Figure (9).

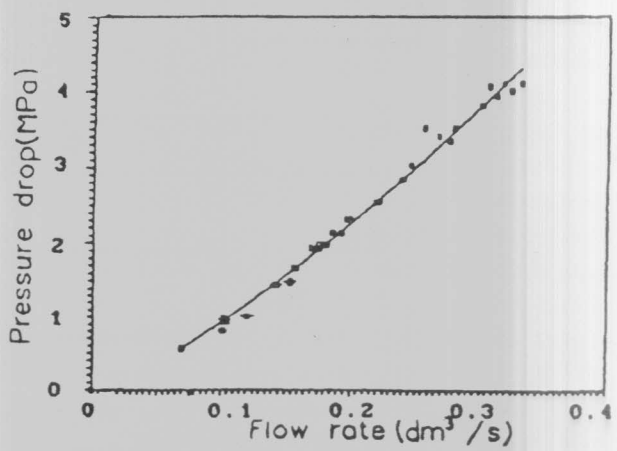

Figure 9. Dependence of the pressure losses in the transmission on the flow rate.

ANALYSIS OF RESULTS

Transient Response of the Closed end Line.

In this part of the work, the dynamic behavior of the transmission line is investigated. The pipe is disconnected from the hydraulic cylinder and its end is plugged. When actuating the electric solenoid of the directional control valve, the main spool displaces, communicating the high pressure oil to the transmission line. The resulting transient pressure variation at the closed end of the line is recorded. The same response is calculated by the simulation program for the line represented by one, two, three and four oil lumps. The experimental and theoretical results, when operating at an inlet pressure level of 5 Mpa, are given in Figure (10).

This figure shows considerable disagreement between the response of the single lump model and the experimental results. The single lump model presents longer time of response, lower damped natural frequency and greater rise time compared with the experimental results. The observed delay in the response is attributed to the delay in the response of directional control valve, Figure (8). When increasing the number of lumps, the theoretical results presented better agreement with the real system response. The transient response of the four lumps model presented good agreement with the experimental results specially on the level of the settling time and the damped natural frequency.

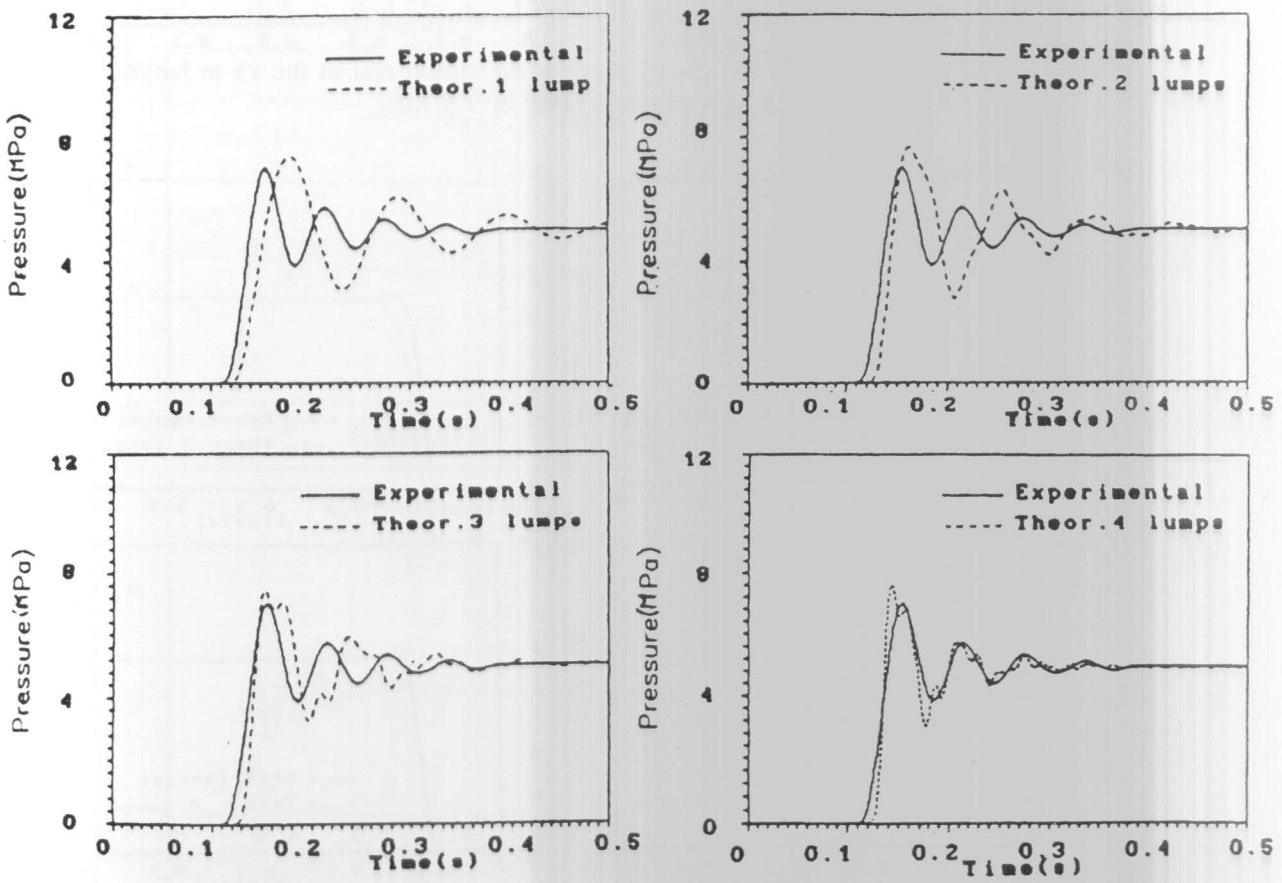

Figure 10. Transient response of the pressure at the closed end of the 15 m length line at an inlet pressure level of 5 MPa.

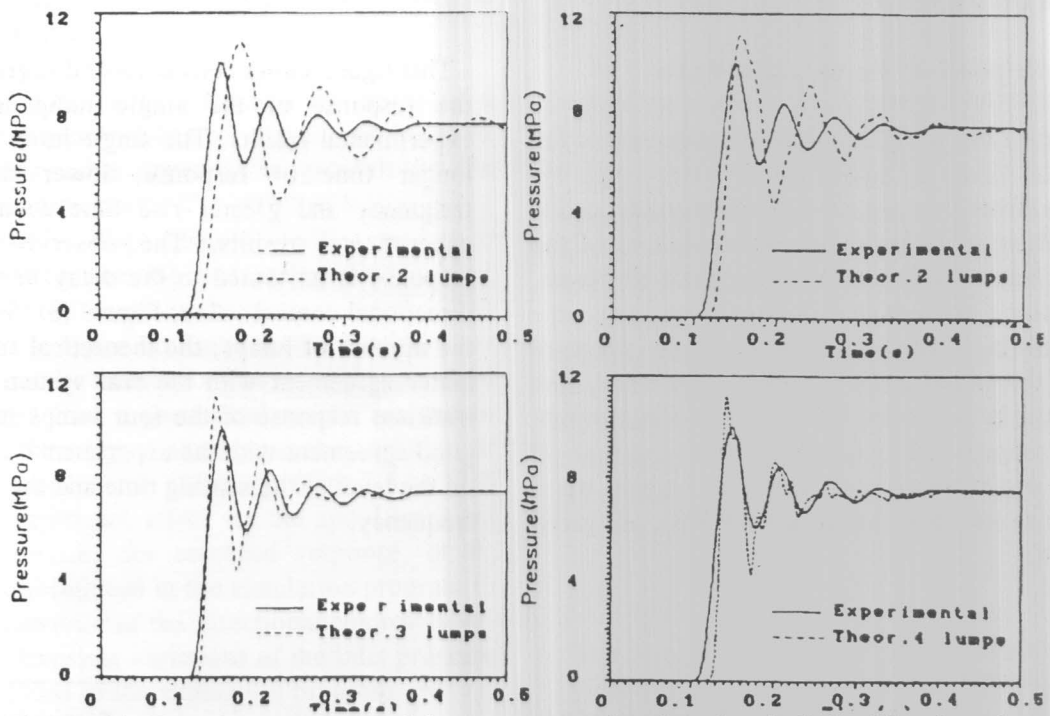

Figure 11. Transient response of the pressure at the closed end of the 15 m length line at an inlet pressure level of 7.5 MPa.

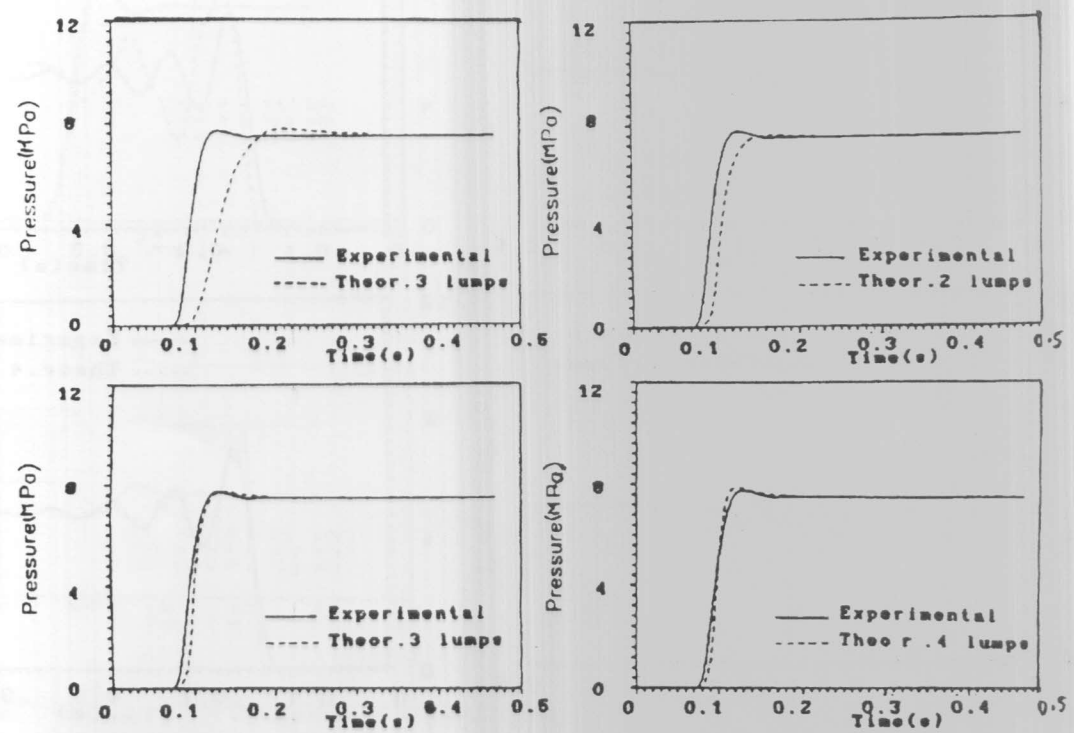

Figure 12. Transient response of the pressure at the closed end of the 2 m length line at an inlet pressure level of 7.5 MPa.

The increase in the inlet pressure to 7.5 Mpa, Figure (11), resulted in a slight increase in the percentage overshoot ratio due to the increase of fluid speeds and the inertia effect. Apart from the difference in the maximum percentage overshoot ratio between the simulation and experimental results, the four lumps model presents satisfactory agreement with the real system behavior. The above mentioned procedure is repeated in Figure (12). The study of this figure confirms the above mentioned observations concerning the good agreement of the simulation and experimental results in case of the four lumps models.

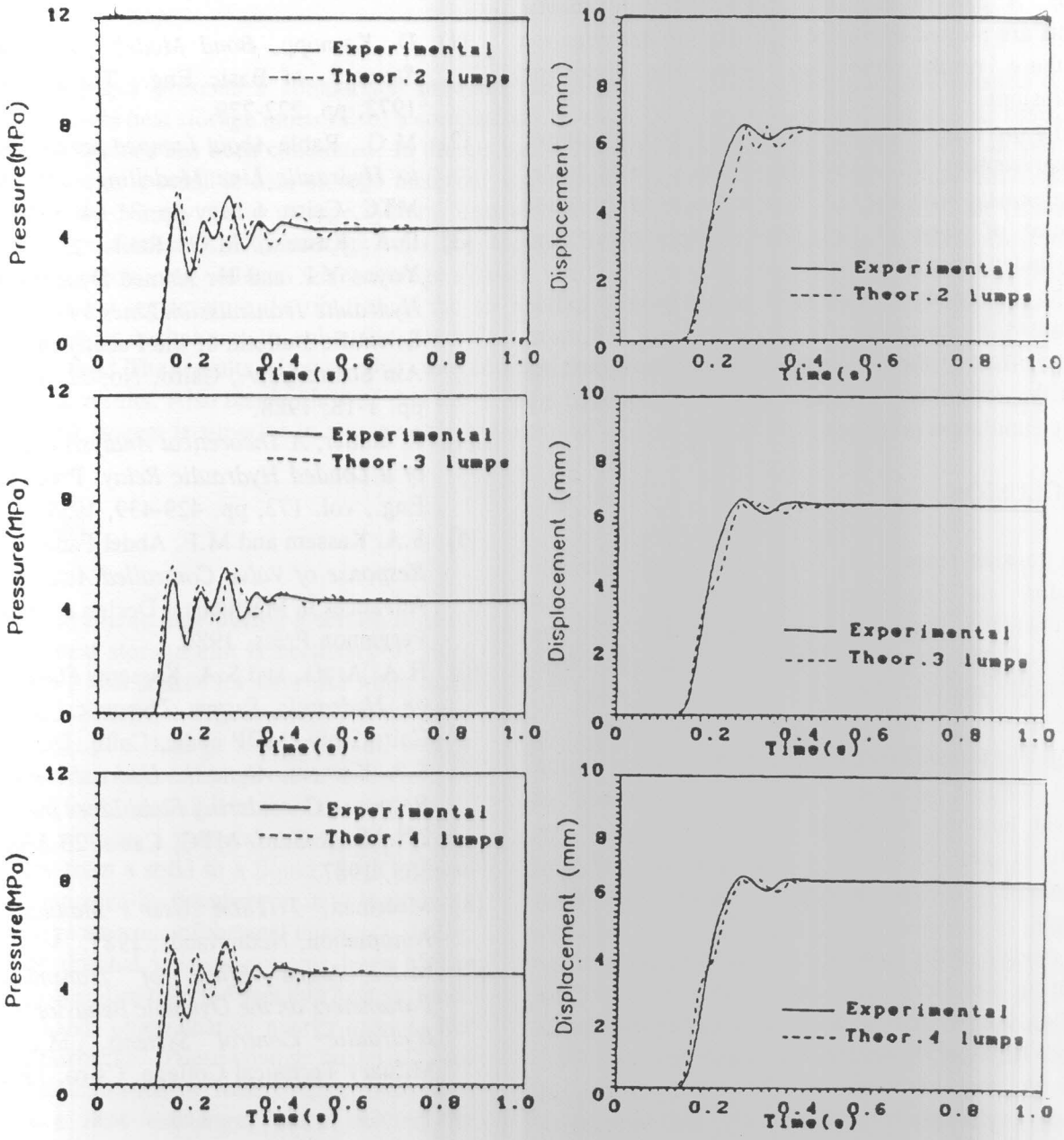

Figure 13. Transient response of the hydraulic cylinder piston displacement and pressure at an inlet pressure level of 5 MPa.

TRANSIENT RESPONSE OF THE HYDRAULIC CYLINDER

The transient response of the hydraulic cylinder is evaluated experimentally and theoretically. This response is calculated, by using the simulation program, when loaded by a constant load. The calculations are carried out at different input pressure levels. A part of the simulations and experimental results are plotted in Figure (13). By the investigation of these results one can reach the following conclusions.

- The increase of the number of fluid to four lumps, representing the transmission line, yields better agreement with the real system behavior from the point of view of the piston displacement and cylinder inner pressure.
- The maximum displacement of the piston rod is limited, by means of a stop tube to be $\leq$ 6.8. mm. The effect of the piston position limiter, appearing in the experimental results is well represented by the simulation program.

CONCLUSION

The transient response of a valve controlled hydraulic cylinder is investigated theoretically and experimentally. A special attention is paid to study the effect of the transmission line dynamics. The theoretical analysis included the development of nonlinear mathematical models representing the system. The transmission line is represented, according to the lumped parameter approach by models of different number of lumps. The simulation of the system is carried out by the treatment of the mathematical model using a digital simulation program.

The models of the transmission line are validated by comparing simulation and experimental results. The and four lumps models are found to represent the transient behavior of the studied closed end lines.

The transient response of the valve controlled hydraulic cylinder is predicted by the simulation program with the piston loaded by a constant load. The simulation results presented good agreement with the experimental results, specially when representing the transmission line by four lumps model, which validates the proposed system model.

The developed simulation program can be used for the optimization of the system parameters as well as the analysis of the dynamic behavior of the valve controlled actuators.

REFERENCES

[1] D. Karnopp, *Bond Models for Fluid Dynamic Stems* J. of Basic Eng., Trans. ASME, Sept. 1972, pp, 222-229.

[2] M.G., Rabie *About Lumped parameter Approach to Hydraulic Line Modelling*, 2nd AME Conf., MTC, Cairo, 6 May pp, 31-64, 1986.

[3] D.A. Kassem, M.G. Rabie, El Adawyee, S., Yoyns Y.I. and H. Ahmed *Dynamic Analysis of Hydraulic Transmission Lines by a Lumped Model* Scientific Bulletin of the Faculty of Engineering, Ain Shams univ., Cairo, No. 22, vol. 2, March, pp. 1-18, 1988.

[4] R. Butler, *A Theoretical Analysis of the Response of a Loaded Hydraulic Relay*, Proc. Inst. Mech. Eng., vol. 173, pp. 429-439, 1959.

[5] S.A. Kassem and M.F. Abdel Fattah, *On the Step Response of Valve Controlled Actuators*, Current Advances in Mechanical Design & Production III, Pergamon Press, 1986.

[6] H.A. Arafa, and S.A. Kassem, *Fluid Line Effects on Hydraulic System Dynamics*, Proc. of 2nd Cairo Univ. MDP conf., Cairo, Dec. 1982.

[7] S.A. Kassem, *About the Hydraulic Actuators Step Response Considering Fluid Lines Inertial Effects*, 2nd ASAR Conf, MTC, Cairo, 23 April pp. 355-365, 1987.

[8] Meerman, *TUTSIM User's Manual*, Meerman Automation, Netherlands, 1987.

[9] M.A. Awad *Effect of Transmission Line Parameters on the Dynamic Behavior Actuators of Hydraulic Control Systems*, M.Sc. Thesis, Military Technical College, Cairo, 1991.

COMPARISON OF MEASURED AND PREDICTED PERFORMANCE OF DIFFERENT HEAT STORAGE SYSTEMS

M.M. El-Kassaby
Mechanical Eng. Dept., Faculty of Engineering,
University of Alexandria, Alexandria, Egypt.

A.A. Ghoneim
Math. & Physics Dept., Faculty of Engineering,
University of Alexandria, Alexandria, Egypt.

ABSTRACT

The present paper presents a comparison between the measured and the predicted performance of different sensible heat storage units. Also, a comparison between the performance of water and air based heat storage systems has been conducted. In the air based systems, natural soil available at Mu'tah site, Jordan is used as a sensible heat storage material. Experimental set up is designed for three different storage systems namely water storage system, unstratified air storage system, and stratified air based system. The performance of the storage units, i.e. the heat accumulated by the storage material (soil in air storage systems, and water in water storage system) is calculated. A computer program is developed to determine the temperature distribution of the air based storage systems. The numerical model uses finite differences techniques to solve the governing equations for both the storage material and the circulating fluid.The results showed that the computer model is in a good agreement with the experimental results. Also results showed that the stratified tank performs better than the unstratified one and the water system is superior in storage energy inspite of its harmful corrosion effect.

INTRODUCTION

Solar energy is available only during a certain time of the day. So, a heat storage unit is necessary to store the energy from a heat source for later use when there is a heat demand. Energy storage is usually in the form of sensible energy of a fluid or solid medium, energy associated with the phase-change of a material, or energy released from reversible chemical reactions.

In latent heat storage, a material undergoes a phase change, usually from a solid to a liquid. Such a phase change is accompanied by the absorption or the release of relatively large amounts of thermal energy. Usually, the latent heat thermal storage systems have higher energy storage densities than the sensible heat systems. On the other hand, phase-change energy storage has two major drawbacks. Phase-change materials are more expensive than rock or water. Also, these units must contain a heat exchanger since neither the circulating fluid is the same as the storage medium as the case in water based system, nor the storage medium is always a solid as the case in the pebble bed storage system.

The main advantages of air based systems are : (1) the availability, and relatively low cost of the storage material, (2) the direct contact between the fluid and the solid material which results in a small temperature gradient, (3) the low thermal conductivity of the solid in the radial direction which reduces the requirement for system insulation, (4) unlimited storage temperature. On the other hand, the main disadvantages of such systems are : (1) large storage volume due to their low heat capacities, (2) large pressure drops which require large fans, (3) charging and discharging can not be done simultaneously [1,2,3].

The main advantages of water based systems are : availability, nontoxicity, high density, high specific heat, and low cost. The major drawbacks of water based systems are freezing or boiling of water, corrosion, and storage temperature is limited to 100°C [3].

In an early trial to use pebble bed as a storage system, Hughes et al [4] had introduced a theoretical model to

use pebble bed, for solar air heating and cooling. In their model they neglected both losses from the storage unit to the surroundings and heat conduction in the direction normal to the flow. In addition, they assumed infinite thermal conductivity for the rock bed in the direction normal to the flow. These simplified assumptions had been modified in the present study.

Mumma and Marvin [5] have reported a straight forward simulation for the behavior of rock bed storage systems. The simulation is based on a one dimensional transient analysis of energy exchange between the air stream and the pebbles, using a finite difference representation. Sowell and Curry [6] modified Mumma and Marvin's model and they reported that Mumma and Marvin's results are generally accurate.

In an attempt to reduce the volume of the pebble bed, Ammar et al [7] had studied theoretically the performance of using a new sensible storage material called Tafla found in Egypt's desert instead of pebble bed. They concluded that Tafla gives a better performance, based on the volume of the storage unit, in comparison with a pebble bed.

One method for making heat more available within the content of sensible heat storage is to use thermal stratification [8,9]. That is was one of the objectives of our study. We designed a stratified tank to check the effect of stratification on the amount of the energy storage.

The main objectives of the present work are :

1. To study the possibility of using an available natural soil at Mu'tah site, Jordan as a sensible heat storage material.
2. To compare between the performance of both air and water based storage systems.
3. To compare between the measured and the predicted performance of the different heat storage systems.

To achieve the previous objectives, the performance of three different storage tanks are examined: water storage tank, and air based system with stratified and unstratified tanks. Air based systems use natural soil available at Mu'tah site, Jordan as a sensible heat storage material. This soil is used because it is cheap and abundant

EXPERIMENTAL SET UP

1. *Configuration of the Unstratified Air Storage System*

The configuration installed to study the performance of the unstratified air tank is shown in Figure (1). The main components are : flat plate collector, storage tank, fans, and valves. The collector area is equal to 0.57 m^2. A solarimeter model TD2086 is used to determine the integrated total radiation on the collector surface over a time interval. Copper-constantan thermocouples are inserted to one of the soil cylinder at different distances longitudinally and at the top of each cylinder as indicated in Figure (2) to measure the soil temperature.

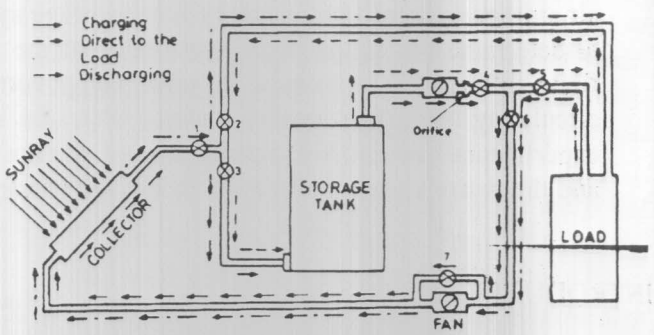

Figure 1. Schematic representation of the solar air heating system for unstratified tank.

The volume of the storage tank is calculated based on the amount of maximum energy which can be stored in the soil (based on the maximum estimated insolation and the maximum estimated collector efficiency). The storage unit consists of a tank packed in the vertical direction with cylindrical tubes. The storage material (i.e. the natural soil) is inside the tubes and the heat transfer fluid flows parallel to it. To have as much storage material as possible, the tank must be closely packed. Due to limited fabrication facilities inside Mu'tah workshop, the minimum diameter of the cylindrical tubes was 10 cm. The storage tank specifications are shown in Figure (2). To insure equal distribution of air around the soil tubes, air enters first through a hole of 1.8 cm in diameter drilled in a ring located at the bottom of the tank and then enters to the storage tank through small holes 3 mm in diameter.

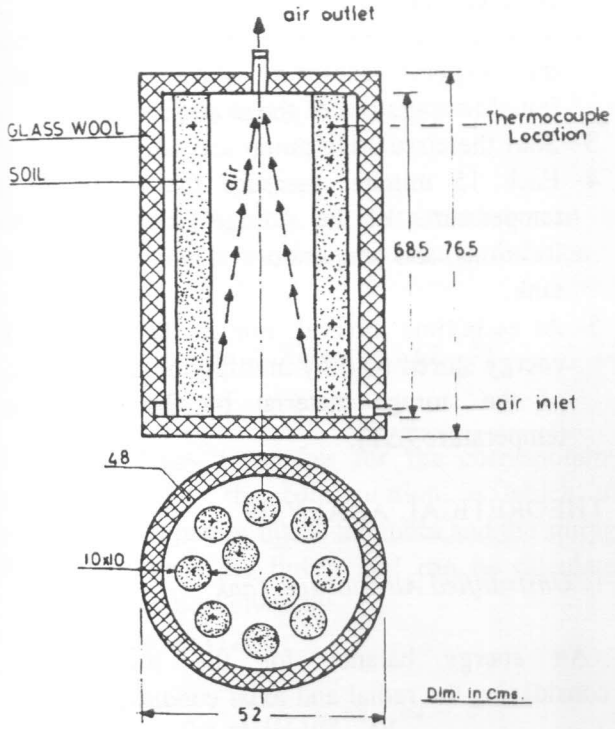

Figure 2. Details of unstratified tank.

In the present work, a natural soil at Mu'tah site, Jordan is used as a sensible heat storage material. The specific heat of the soil is measured using heat capacity calorimeter manufactured by PHYME company, Germany and was found to be equal to 1.013 kJ/kg K.

The transient probe method is used to determine the thermal conductivity of the soil. The thermal conductivity is determined from a record of probe temperature versus time. The porosity greatly influences the density and the thermal conductivity of the soil. In this study, the measurements were repeated several times and each time the porosity of the dried sample is determined. The thermal conductivity and the density of the soil corresponding to porosity equal to 24% (the porosity of the soil used in the storage tank) are found to be 6.4 W/mK and 1960 kg/m^3, respectively.

Charging the tank (i.e. storing energy) is achieved by closing valves no. 2, 5, and 7 and start the fan located before valve no. 4 (as indicated by solid arrows in Figure (1)). To discharge the tank, close valves no. 1, and 6 and start the first fan only (as indicated by dashed arrows in Figure (1)). If the system is used directly for heating load, valves 3 and 4 are closed and the fan located parallel to valve no. 7 is operated, while the first one is closed (as indicated by center line arrows in Figure (1)).

2. *Configuration of the Stratified Air Storage System*

The configuration chosen for studying the performance of the stratified air tank is shown in Figure (3). The same design criteria for the unstratified air tank is followed again, but we tried to make the temperature distribution more stratified by entering the air from three locations, and collecting air from other three locations. In other words, the stratified tank is a three small unstratified tanks. This was done to see the effect of stratification on the collection efficiency. The stratified air tank specifications are presented in Figure (4). The same steps as in the unstratified air tank are followed to charge and discharge the stratified air tank.

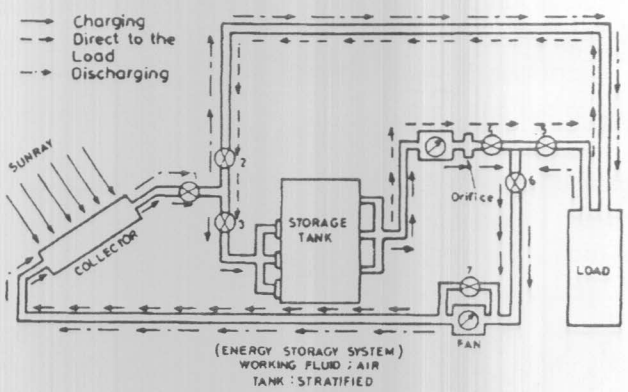

Figure 3. Schematic representation of the solar air heating system for stratified tank.

3. *Configuration of the Water Storage System*

The configuration used to study the performance of the water storage system is shown in Figure (5). The main components are: flat plate collector, water storage tank, pump, and valves. The collector area is equal to 0.57 m^2 . The volume of the storage tank is calculated based on the maximum energy that can be stored by water. For optimum surface area the diameter of the storage tank must equal its length. This gives a storage tank of radius equal to 0.38 m. Charging the tank is done by closing valves no. 1, 4, and 5 and start the pump. To discharge the tank, close

valves no. 2, and 3 and leave valves 4, and 5 open. Then switch off the pump.

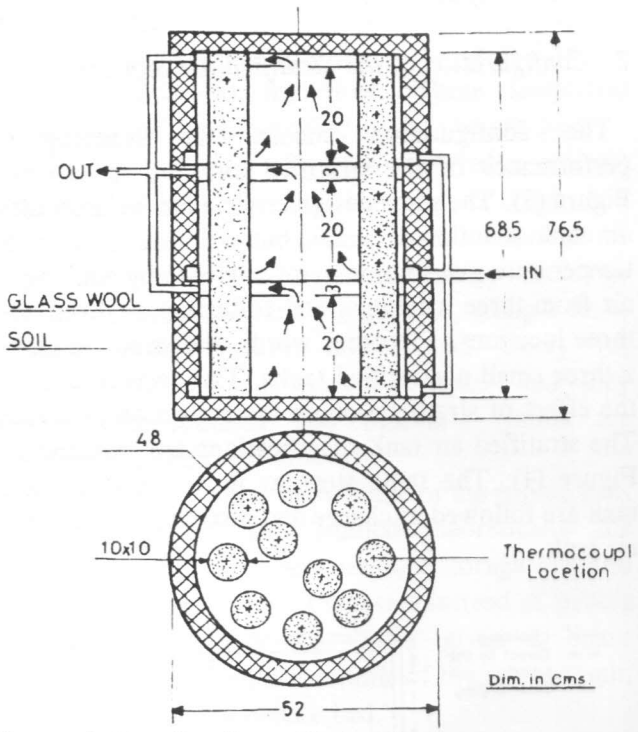

Figure 4. Details of stratified tank.

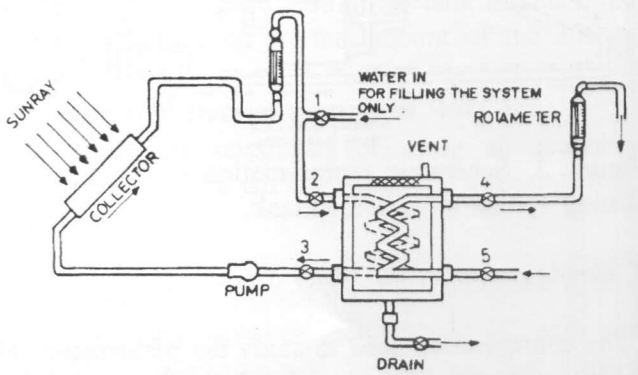

Figure 5. Schematic representation of the solar storage system.

Experimental Procedure

To compare between the systems explained above, all the systems are examined under the same climatic conditions using the following steps :

1- Put the solarimeter receiver on the top of the collector surface.
2- Measure the temperature of the storage materials at the different locations which is considered the initial temperature of the storage material.
3- Start the circulating pump and fans.
4- Each 15 minute, measure the fluid flow rate, temperatures of the storage material at different locations, and temperature at inlet and outlet of the tank.
5- At each time interval, one can calculate the total energy stored (Q_2) by multiplying the heat capacity of the storage material by the total raise in temperature (ΔT).

THEORETICAL ANALYSIS

1. *Unstratified Air Storage Tank*

An energy balance for the storage material considering the radial and axial conduction, yields

$$\frac{\partial T}{\partial t}=\frac{k}{\rho c_p}\frac{\partial^2 T}{\partial r^2}+\frac{k}{\rho c_p r}\frac{\partial T}{\partial r}+\frac{k}{\rho c_p}\frac{\partial^2 T}{\partial z^2} \qquad (1)$$

An energy balance for the circulating fluid yields

$$\rho_f A_f c_f \frac{\partial T_f}{\partial t}+mc_f\frac{\partial T_f}{\partial z}=UP(T-T_f)+U'P_f(T_{env}-T_f) \qquad (2)$$

The total heat loss coefficient from the storage unit to the surroundings, U',is assumed to be equal to 0.416 W/m^2 K [10]. Adiabatic boundary conditions are assumed at the bottom and the top of the storage unit, i.e. the heat flow through the upper and lower surfaces is equal to zero, and there is no heat flow through the axis of the cylinder.

The value of the heat transfer coefficient, U, describing the energy flow between the heat transfer fluid and the storage material depends on the type of the flow, i.e. laminar (Re < 2200) or turbulent flow (Re > 2200). The Nusselt number, Nu, can be calculated from the empirical relations given by Rohsenow et al. [11] assuming a constant surface temperature. For laminar flow, the Nusselt number can be expressed as :

be expressed as :

$$Nu=3.66+4.12(\frac{D_h}{r_i}-0.205)^{0.569} \quad (3)$$

For turbulent flow, the Nusselt number can be calculated from the following empirical correlation :

$$\frac{Nu}{Nu'}=1.08-0.794\exp[-1.62\frac{D_h}{r_i}] \quad (4)$$

Nu', is the Nusselt number for the corresponding configuration (i.e. the configuration in which the circulating fluid passes inside the tubes and the storage material surrounds the fluid). Nu' can be calculated from the correlation given by
Dittus and Boelter [12] :

$$Nu'=0.023Re^{0.8}Pr^{0.4} \quad (5)$$

Solution Method

A computer program compatible with TRNSYS (transient simulation program) is developed to simulate the performance of the heat storage unit. TRNSYS [10] is a transient simulation program developed at Solar Energy Laboratory at University of Wisconsin-Madison to simulate the performance of the different components of the solar systems.
To simplify the computer program, the governing equations (1, and 2) are rewritten in a nondimensional form using the following nondimensional groups :

$$\theta=\frac{T}{T^*}, \qquad \theta_f=\frac{T_f}{T^*}, \qquad \theta_{env}=\frac{T_{env}}{T*} \quad (6)$$

$$V=\frac{r_i}{L}, R=\frac{r}{r_i}, W=\frac{\rho_f A_f c_f}{\rho A c_p}, Y=\frac{U'P_f}{UP} \quad (7)$$

$$\xi=\frac{UPz}{mc_f}, Bi=\frac{Ur_i}{k}, Fo=\frac{kt}{\rho c r_i^2}, NTU=\frac{UPL}{mc_f} \quad (8)$$

Substitution of these nondimensional quantities into equations (1), and (2) gives the following nondimensional equations for both the storage material and the fluid:

$$\frac{\partial\theta}{\partial Fo}=[\frac{\partial^2\theta}{\partial R^2}+\frac{1}{R}\frac{\partial\theta}{\partial R}]+V^2(NTU)^2\frac{\partial^2\theta}{\partial\xi^2} \quad (9)$$

$$\frac{\partial\theta_f}{\partial Fo}=\frac{2Bi}{W}[(\theta-\theta_f)+Y(\theta_{env}-\theta_f)-\frac{\partial\theta_f}{\partial\xi}] \quad (10)$$

Finite difference techniques are used to solve equations (9), and (10). The storage unit is divided into N nodes in the axial direction (i.e. the direction parallel to the fluid flow), and M nodes in the radial direction (i.e. direction normal to the fluid flow). The stability and the accuracy of the present numerical solution depend upon the time step (Δt), the number of the axial nodes (N), and the number of the radial nodes (M). First of all, a parametric study is performed to determine the effect of the time step, and the number of the axial and radial nodes values on the results.
The variation of the heat stored with time is calculated using different values of time step, number of the axial and radial nodes. Generally there is no significant variation in the stored energy with increasing the number of the radial points above 5 (i.e. M=5) or with increasing the number of the axial points above 10 (i.e. N=10). Also, stability and acceptable accuracy conditions are achieved for time step values less than or equal to 7 minutes.
The time step required for the stability of the storage tank subroutine (Δt) is several times smaller than the time step required for other TRNSYS subroutines (Δt_{TR}). This problem is solved by running TRNSYS at the optimum time step (usually 15 minutes) and subdividing it within the storage tank subroutine time step (Δt). In general (Δt_{TR}) does not exactly equal an integer number of (Δt). Introducing a number, N_s, which is the first integer greater than ($\Delta t_{TR}/\Delta t$), the time step of the storage tank subroutine can now be recalculated from the following equation :

$$\Delta t' = \frac{\Delta t_{TR}}{N_s} \qquad (11)$$

For every TRNSYS time step, the equations in the storage tank subroutine are solved N_s times. This method saves a large computational time in comparison with the other option of running TRNSYS subroutines with the smaller time step of the storage tank subroutine. Finally, another sensitivity study is performed after incorporating the storage tank subroutine into TRNSYS. An energy balance for the storage tank subroutine is conducted for each simulation. The present results showed a closure of 0.4-2%.

2. STRATIFIED AIR STORAGE TANK

For stratified air tank, the storage tank is divided into three equal unstratified tanks, and the computer program used to simulate the unstatified tank is used again for each unstratified tank.

3. WATER STORAGE TANK

For the water storage tank, we used the stratified storage tank subroutine (Type 4) contained in the TRNSYS library to simulate the performance of the water storage tank. The performance of the stratified tank is modelled by assuming that the tank is consisted of N fully-mixed equal value segments. The flow stream enters the closest node to it in temperature. With ten nodes (i.e. N=10), a maximum degree of stratification is reached.

RESULTS AND DISCUSSION

The measurements are carried out continuously for twenty days. A sample of experimental results taken in a sunny day, during April 1990, are compared with the corresponding one obtained from the theoretical model in Figures (6) through (9). In Figure (6), the total heat gained by the storage material ($Q_2 = m\ c_p\ \Delta t$) versus time for the water storage tank is plotted. From th figure, it is clear that the predicted results are in good agreement with the experimental results, with a maximum error of about 15%, which is considere within the range of the experimental error.

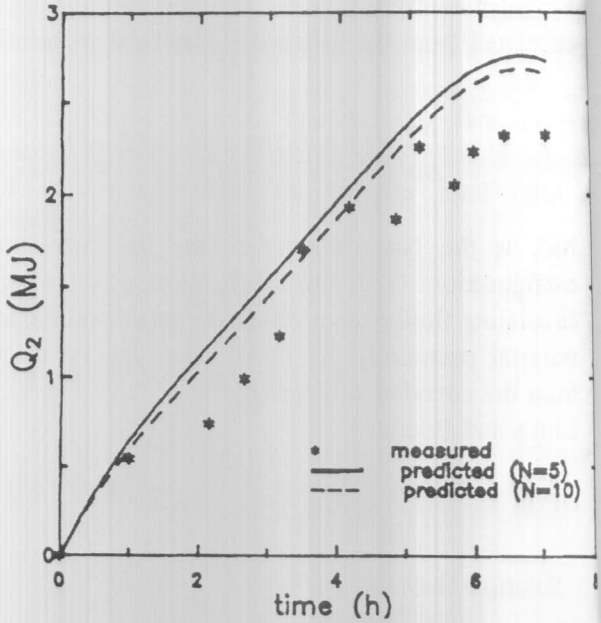

Figure 6. Variation of the stored energy with time for water storage system (22/4/1992).

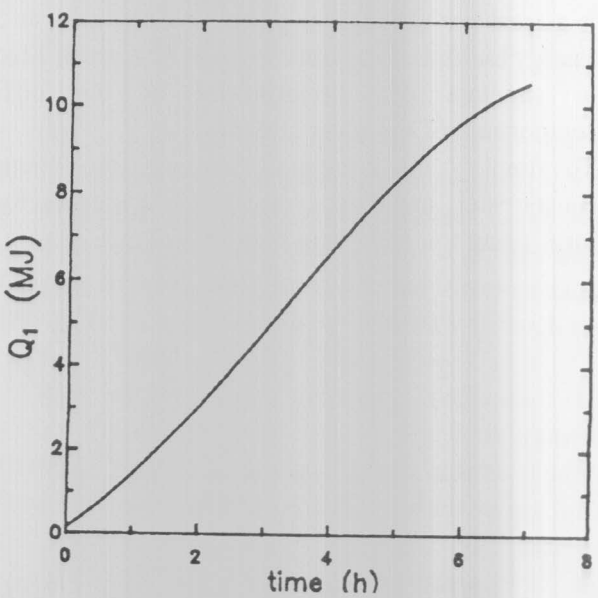

Figure 7. The integrated solar insolation incident on the collector surface (22/4/1990).

Figure (7) shows the integrated solar insolation incident on the collector surface ($Q_1 = A_c \int I\, dt$) versus time. It is worth to mention that the starting time was 9 am, that is why the rate of solar insolation starts to increase rapidly and starts to decrease after 6 hours of operation when the solar insolation starts to decrease.

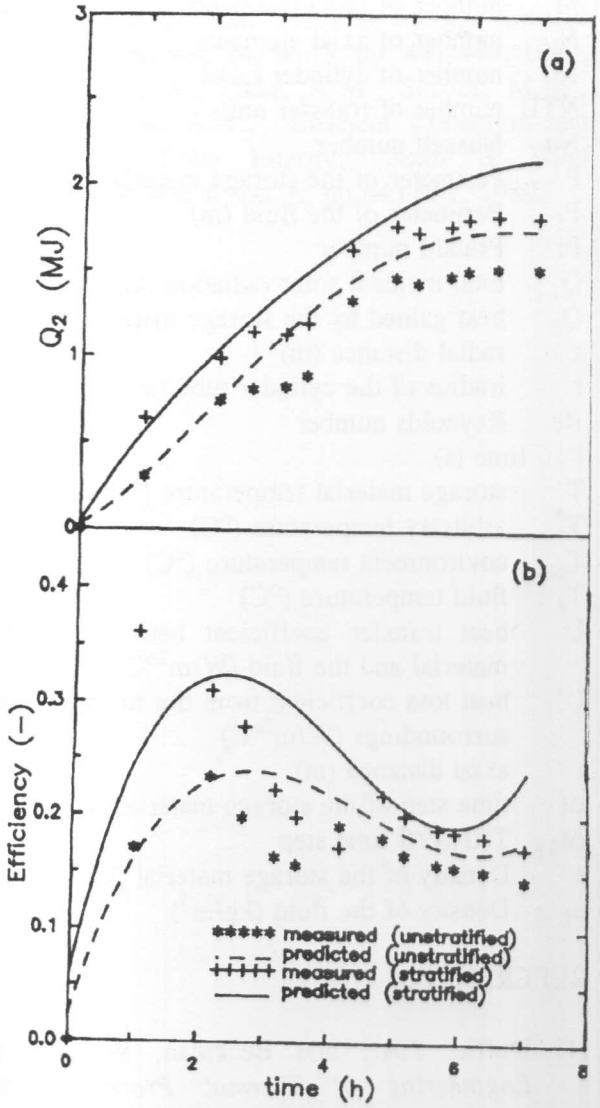

Figure 8. Comparison between stratified and air tank.
a- heat gained by storage material
b- system efficiency.

Figure (8) shows the comparison between stratified and unstratified air storage tanks. It is clear that the heat gained by the stratified air tank at the end of the charging period is higher than that gained by unstratified tank by around 25%. The efficiency of the stratified tank is greater by an average of about 5% than that of unstratified tank. The reason of that is in stratified tank, the air movement across the tubes takes place in a shorter distance, which means that the chance for the particles of the air to move parallel to the mud tube becomes smaller and the chance to move across the tube becomes higher (see Figure 4). This improves the heat transfer coefficient between air and the storage material. While in stratified air tank there is a great chance for air particles to move parallel to the storage material for a longer time reducing the heat transfer coefficient.

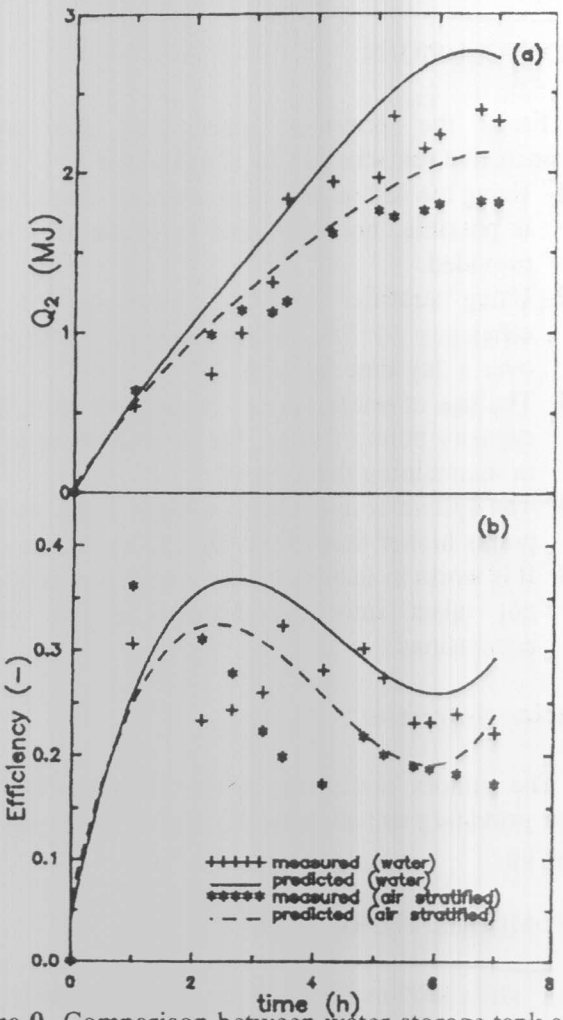

Figure 9. Comparison between water storage tank and air stratified tank.
a- heat gained by storage material
b- system efficiency.

Also, it is clear that the minimum efficiency gained is at noon time, where the system temperature is at its highest temperature, meaning the highest heat loss at this instant. There is around 20 m long of insulated tube used in air tank. This means that the heat loss is an important factor in determining the efficiency of the system.

The comparison between the water storage tank and the stratified air tank is presented in Figure (9). It is clear from the figure that the water storage tank performs much better than the air tank. The heat storage in the water tank is higher than that of stratified air tank by an amount of about 0.8 MJ, which represents around 30% of the total heat stored. This is due to the superiority of water properties over air. Similar results are obtained for all the other days.

CONCLUSIONS

From the previous discussion, the following conclusive remarks can be summarized :

1- Using the soil as a storage material instead of water is possible, but additional collector area must be provided.
2- Using stratified air tank increases the system efficiency by 5% and the amount of stored heat over a day time by 25%.
3- The use of water system is superior from the heat capacity point of view, but there is some problems in maintaining the system.
4- The system is not sensitive much to the number of points higher than 10 (in the theoretical model).
5- It is worth to mention that economic evaluations are not taken into consideration in all previous conclusions.

Acknowledgement

The authors would like to thank Mu'tah University for providing and allowing the use of the experimental set up.

NOMENCLATURE

A	cross sectional area of the storage material (m^2)
A_c	collector area (m^2)
A_f	fluid area (m^2)
Bi	Biot number
c_f	specific heat of the circulating fluid (kJ/kgK)
c_p	specific heat of the storage material (kJ/kgK)
D_h	hydraulic diameter (m)
Fo	Fourier number
I	total solar radiation (W/m^2)
k	thermal conductivity of storage material (W/mK)
k_f	thermal conductivity of the fluid (W/mK)
L	storage unit length in the flow direction (m)
m	fluid mass flow rate (kg/s)
M	number of radial elements
N	number of axial elements
N_c	number of cylinder tubes
NTU	number of transfer units
Nu	Nusselt number
P	Perimeter of the storage material (m)
P_f	Perimeter of the fluid (m)
Pr	Prandtl number
Q_1	total incident solar radiation (kJ)
Q_2	heat gained by the storage material (kJ)
r	radial distance (m)
r	iradius of the cylinder tube (m)
Re	Reynolds number
t	time (s)
T	storage material temperature (°C)
T^*	arbitrary temperature (°C)
T_{env}	environment temperature (°C)
T_f	fluid temperature (°C)
U	heat transfer coefficient between the storage material and the fluid ($W/m^2°C$)
U'	heat loss coefficient from the storage unit to the surroundings ($W/m^2°C$)
z	axial distance (m)
Δt	time step of the storage material (s)
Δt_{TR}	TRNSYS time step
ρ	Density of the storage material (kg/m^3)
ρ_f	Density of the fluid (kg/m^3)

REFERENCES

[1] Duffie, J.A., and Beckman, W.A., " *Solar Engineering of Thermal Processes*," Wiley Interscience, New York, 1980.
[2] Howell, Bannerot, Vliet, " *Solar Thermal Energy Systems*," Mc Graw Hill Book Company, 1982.
[3] Garg, H.P., "*Advances in Solar Energy Technology*," D. Reidel Publishing Company, Holland, 1987.
[4] Hughes, P.J., Klein, S.A., and Close, D.J.,